Journal of Thermal Analysis, Vol. 24 (1982) 233–260

ANALYSIS OF THE LATTICE THERMAL CONDUCTIVITY AND PHONON-PHONON SCATTERING RELAXATION RATE: APPLICATION TO Mg_2Ge AND Mg_2Si

A. H. AWAD and K. S. DUBEY

Department of Physics, College of Science, University of Basrah, Basrah — Iraq

(Received February 3, 1982)

The lattice thermal conductivities of Mg_2Ge and Mg_2Si have been analysed in the entire temperature range 2–1000 K in the frame of a new expression for the phonon-phonon scattering relaxation rate proposed by Dubey as

$$\tau_{3ph}^{-1} = (B_{N,I} + B_{U,I}\, e^{-\theta/\alpha T})\, g(\omega) T^{m_I(T)} + (B_{N,II} + B_{U,II}\, e^{-\theta/\alpha T})\, g(\omega) T^{m_{II}(T)}$$

based on the Guthrie classification of the phonon-phonon scattering events, and a very good agreement has been obtained between the calculated and experimental values of the lattice thermal conductivity for both samples in the entire temperature range of the study. The separate percentage contributions due to three-phonon normal and umklapp processes towards the three-phonon scattering relaxation rate have also been studied. The role of the four-phonon processes has been included in the present analysis.

The lattice thermal conductivities of insulators and semiconductors have been studied by a number of workers [1–10] and it is well established that phonon-phonon scattering plays a very important role in the analysis of the lattice thermal conductivity of a sample. The three-phonon scattering processes dominate over other processes at high temperatures. At the same time, these processes are not negligibly small at low temperatures and play an important role in the vicinity of the conductivity maxima. However, due to the complex structure of the Brillouin zone and the strong temperature-dependence of the phonon distribution function, the three-phonon scattering relaxation rate involves a complicated dependence on the phonon frequency as well as on the temperature. As a result, even at present we lack an exact analytical expression for this. For practical purposes, there is a need to express the three-phonon scattering relaxation rate by simple relations as a function of the phonon frequency and temperature. Several workers [1–7, 11–14] studied the phonon-phonon scattering processes by dividing them into groups: normal processes (N-processes), in which momentum is conserved, and umklapp processes (U-processes), in which momentum is not conserved, and they expressed the three-phonon scattering relaxation rates $\tau_{3ph,N}^{-1}$ and $\tau_{3ph,U}^{-1}$ due to N- and U-processes, respectively, as simple functions of the phonon frequency and temperature, as reported in Table 1. The expressions in Table 1 have been used by a number of workers [15–20] to analyse the lattice thermal conductivities of the different samples in the frame of the combined scattering relaxation rates (see Table 2) at high as well as at low temperatures, and it is reported that

Table 1

The three-phonon scattering relaxation rates. In these expressions, B's are constants and are known as the scattering strenghts of the respective processes, α is constant, θ is the Debye temperature and q_{max} is the zone boundary of the first Brillouin zone. Suffixes T and L stand for transverse and longitudinal phonons, respectively, and suffixes N and U refer to three-phonon normal and umklapp processes, respectively

Three-phonon processes τ_{3ph}^{-1}	Relaxation rate	
Normal processes [11] (N-processes):	$\tau_{3ph,N}^{-1}$	
Transverse:	$\tau_{TN}^{-1} = B_T \omega T^4$	at low temperature
Longitudinal:	$\tau_{LN}^{-1} = B_L \omega^2 T^3$	at low temperature
Transverse:	$\tau_{TN}^{-1} = B'_T \omega T$	at high temperature
Longitudinal:	$\tau_{LN}^{-1} = B'_L \omega^2 T$	at high temperature
Umklapp processes (U-processes):	$\tau_{3ph,U}^{-1}$	
Klemens [13] (longitudinal):	$\tau_{L,U}^{-1} = B_U \omega^2 T^3 e^{-\Theta/\alpha T}$	at low temperature
Klemens [12] (transverse):	$\tau_{T,U}^{-1} = B'_U \omega T^3 e^{-\Theta/\alpha T}$	at low temperature
Holland [2] (transverse):	$\tau_{T,U}^{-1} = B_{T,U} \omega^2 / \mathrm{Sin}\hbar(h\omega/K_B T)$	$1/2q_{max} - q_{max}$
	$\tau_{T,U}^{-1} = 0$	$0 - 1/2q_{max}$
Callaway [1]:	$\tau^{-1} = B_U \omega^2 T^3$	$0 - q_{max}$
	$\tau^{-1} = B_U \omega^2 T$	at high temperature
Joshi and Verma [3] (transverse):	$\tau_{3ph,T}^{-1} = B_T \omega T^m$	$0 - q_{max}$
(longitudinal):	$\tau_{3ph,L}^{-1} = B_L \omega^2 T^m$	$0 - q_{max}$
SDV [4, 5] (transverse):	$\tau_{3ph,T}^{-1} = B_{T,I} \omega T^{m_{T,I}^{(T)}} e^{-\Theta/\alpha T}$	$0 - q_{max}$
(longitudinal):	$\tau_{3ph,L}^{-1} = B_{L,I} \omega^2 T^{m_{L,I}^{(T)}} e^{-\Theta/\alpha T} + B_{L,II} \omega^2 T^{m_{L,II}^{(T)}} e^{-\Theta/\alpha T}$	$0 - q_{max}$
Dubey and Misho [6] (transverse):	$\tau_{3ph,T}^{-1} = (B_{TN} + B_{TU} e^{-\Theta/\alpha T}) \omega T^m$	$0 - q_{max}$
(longitudinal):	$\tau_{3ph,L}^{-1} = (B_{LN} + B_{LU} e^{-\Theta/\alpha T}) \omega^2 T^m$	$0 - q_{max}$
Dubey [33] (transverse):	$\tau_{3ph,T}^{-1} = (B_{TN,I} + B_{TU,I} e^{-\Theta/\alpha T}) \omega T^{m_{T,I}^{(T)}}$	$0 - q_{max}$
(Present work) (longitudinal):	$\tau_{3ph,L}^{-1} = (B_{LN,I} + B_{LU,I} e^{-\Theta/\alpha T}) \omega^2 T^{m_{L,I}^{(T)}} + (B_{LN,II} + B_{LU,II} e^{-\Theta/\alpha T}) \omega^2 T^{m_{L,II}^{(T)}}$	$0 - q_{max}$

these expressions give a good response to the experimental data on the lattice thermal conductivity.

The three-phonon scattering relaxation rates were further studied by Guthrie [31, 32] by dividing the phonon-phonon scattering events into two classes: class I

Table 2

The combined scattering relaxation rates. In these expressions, ω_1 and ω_2 are the transverse phonon frequencies at $1/2q_{max}$ and q_{max}, respectively, ω_3 and ω_4 are the same for longitudinal phonons, ω_D is the Debye frequency, τ_B^{-1} and τ_{pt}^{-1} are the boundary and point-defect scattering relaxation rate, respectively, and the other terms have the same meanings as stated in Table 1

	Combined scattering relaxation rates τ_c^{-1}	Frequency range
Callaway [1]	$\tau_c^{-1} = \tau_B^{-1} + \tau_{pt}^{-1} + (B_1 + B_2)\omega^2 T^3$	$0 - \omega_D$
Holland [2]	$\tau_{c,T}^{-1} = \tau_B^{-1} + \tau_{pt}^{-1} + B_{TN}\omega T^4$	$0 - \omega_1$
	$\tau_{c,T}^{-1} = \tau_B^{-1} + \tau_{pt}^{-1} + B_{TU}\omega^2/\mathrm{Sin}\hbar(h\omega/K_B T)$	$\omega_1 - \omega_2$
	$\tau_{c,L}^{-1} = \tau_B^{-1} + \tau_{pt}^{-1} + B_L\omega^2 T^3$	$0 - \omega_4$
Joshi and Verma [3]	$\tau_{c,T}^{-1} = \tau_B^{-1} + \tau_{pt}^{-1} + B_T\omega T^m$	$0 - \omega_2$
	$\tau_{c,L}^{-1} = \tau_B^{-1} + \tau_{pt}^{-1} + B_L\omega^2 T^m$	$0 - \omega_4$
	(m = 1, 2, 3 or 4, depending on the temperature range)	
SDV model [4, 5]	$\tau_{c,T}^{-1} = \tau_B^{-1} + \tau_{pt}^{-1} + B_{T,I}\omega T^{m_{T,I}(T)} e^{-\Theta/\alpha T}$	$0 - \omega_2$
	$\tau_{c,L}^{-1} = \tau_B^{-1} + \tau_{pt}^{-1} + B_{L,I}\omega^2 T^{m_{L,I}(T)} e^{-\Theta/\alpha T}$	
	$+ B_{L,II}\omega^2 T^{m_{L,II}(T)} e^{-\Theta/\alpha T}$	$0 - \omega_4$
Dubey and Misho [6]	$\tau_{c,T}^{-1} = \tau_B^{-1} + \tau_{pt}^{-1} + (B_{TN} + B_{TU}e^{-\Theta/\alpha T})\omega T^m$	$0 - \omega_2$
	$\tau_{c,L}^{-1} = \tau_B^{-1} + \tau_{pt}^{-1} + (B_{LN} + B_{LN}e^{-\Theta/\alpha T})\omega^2 T^m$	$0 - \omega_4$
	m = 1, 2, 3 or 4 for transverse phonons, depending on temperature range, and m = 1, 2 or 3 for longitudinal phonons, depending on temperature range.	
Dubey [33]	$\tau_{c,T}^{-1} = \tau_B^{-1} + \tau_{pt}^{-1} + (B_{TN,I} + B_{TU,I}e^{-\Theta/\alpha T})\omega T^{m_{T,I}(T}$	$0 - \omega_2$
(Present Work)	$\tau_{c,L}^{-1} = \tau_B^{-1} + \tau_{pt}^{-1} + (B_{LN,I} + B_{LU,I}e^{-\Theta/\alpha T})\omega^2 T^{m_{L,I}(T)}$	
	$+ (B_{LN,II} + B_{LU,II}e^{-\Theta/\alpha T})\omega^2 T^{m_{L,II}(T)}$	$0 - \omega_4$

events, in which the carrier phonon is annihilated by combination, and class II events, in which the carrier phonon is annihilated by splitting. According to Guthrie [31], the scattering relaxation rate due to each class of events is of the form

$$\tau_{3ph}^{-1} \propto g(\omega)f(T) \tag{1}$$

where $f(T) = T^{m(T)}$, $m(T)$ is a continuous function of the temperature T, and $g(\omega)$ is the frequency-dependence of the scattering relaxation rate. Recently, considering the role of the three-phonon N- and U-processes, and following the Guthrie classification of the phonon-phonon scattering events, Dubey [33] studied the lattice thermal conductivity of a sample by proposing a new expression for the three-phonon scattering relaxation rate as

$$\tau_{3ph}^{-1} = (B_{N,I} + B_{U,L} e^{-\theta/\alpha T}) g(\omega) T^{m_I(T)} + (B_{N,II} + B_{U,II} e^{-\theta/\alpha T} g(\omega) T^{m_{II}(T)} \quad (2)$$

The terms are explained in the following section.

The aim of the present work is to analyse the lattice thermal conductivities of Mg_2Ge and Mg_2Si in the entire temperature range 2–1000 K in the frame of the expression for the three-phonon scattering relaxation rate recently proposed by Dubey. The total lattice thermal conductivities of both samples Mg_2Ge and Mg_2Si have been calculated by estimating the contributions due to transverse and longitudinal phonons separately. The separate percentage contributions due to transverse and longitudinal phonons towards the total lattice thermal conductivity have been reported for both samples in the entire temperature range of the study. The variation of the temperature exponent $m(T)$ used in the present analysis with temperature has been studied for transverse and longitudinal phonons for both Mg_2Ge and Mg_2Si in the entire temperature range 2–1000 K. The percentage contributions due to three-phonon N-processes and U-processes towards the phonon-phonon scattering relaxation have been estimated for transverse and longitudinal phonons, to see their roles in the analysis of the lattice thermal conductivity of a sample. To study the importance of the phonon-phonon scattering events in more detail, the percentage contribution of the three-phonon scattering relaxation rate towards the combined scattering relaxation rate has been calculated for the different values of the phonon frequency $\omega = \frac{1}{4}\omega_{max}, \frac{1}{2}\omega_{max}, \frac{3}{4}\omega_{max}$ and ω_{max} for transverse and for longitudinal phonons for both samples, Mg_2Ge and Mg_2Si. To see the goodness of the present analysis, a comparative study of the present analysis with the earlier studies is reported. The contribution of the four-phonon scattering processes has been included to estimate the lattice thermal conductivity at high temperatures.

A short feature of the Dubey approach to the lattice thermal conductivity

There can be many phonon scattering processes that lead to the lattice thermal resistivity of a sample. The phonon-phonon scattering processes dominate over other processes at high temperatures and these processes can not be ignored at low temperatures either. They play an important role even in the vicinity of the conductivity maxima. It is difficult to express the three-phonon scattering relaxation rate τ_{3ph}^{-1} as a simple relation, due to the complicated structure of the Brillouin zone, as well as the strong temperature-dependence of the phonon distribution function. To analyse the experimental data on the lattice thermal conductivity, a number of workers [1–7, 11–14] studied the phonon-phonon scattering processes and tried to express the three-phonon scattering relaxation rate τ_{3ph}^{-1} in the form of a simple relation as a function of the phonon frequency ω and the tem-

perature T for the three-phonon N- and U-processes as reported in Table 1. From Table 1, it is clear that the frequency-dependence of τ_{3ph}^{-1} is ω for transverse phonons and ω^2 for longitudinal phonons. It is also clear that the expression for τ_{3ph}^{-1} for transverse phonons is different from that for longitudinal phonons. It should be noted that the Callaway [1] expression is an exception to this, due to the fact that he could not make any distinction between transverse and longitudinal phonons. From this Table, it can also be seen that the expression for τ_{3ph}^{-1} for U-processes consists of an exponential factor. Using the expressions reported in Table 1, the lattice thermal conductivities of a number of samples have been studied [15–30] at low and at high temperatures in the frame of the combined scattering relaxation rates as given in Table 2.

As stated earlier, according to Guthrie [31], the phonon-phonon scattering relaxation rate can be studied by dividing the phonon-phonon scattering events into two classes: class I events, in which the carrier phonon is annihilated by combination, and class II events, in which the annihilation of the carrier phonon takes place by splitting; the scattering relaxation rates for each class of events are the form

$$\tau_{3ph}^{-1} \propto g(\omega) T^{m(I)} \tag{3}$$

where $g(\omega)$ is the frequency-dependence of τ_{3ph}^{-1} and is the same as reported by Herring [11], i.e. $g(\omega) = \omega$ for transverse phonons and ω^2 for longitudinal phonons. The temperature exponent $m(T)$ is a continuous function of temperature T. Guthrie [31, 32] commented on the use of the Herring [11] relations $\tau_{3ph}^{-1} \propto T^4$ and $\tau_{3ph}^{-1} \propto T^3$ for transverse and longitudinal phonons, respectively, at high temperatures, and suggested that these relations are valid only at low temperatures. It is needed to be stated that Guthrie [31] could not give any analytical expression for the exact value of $m(T)$, except that he reported the extreme values of $m(T)$ as:

For class I events:

$$[m(T)]_{max} = X_{max}[2(e^{x_{max}} - 1)^{-1} + 1.0] - 1.0 \tag{4}$$

$$[m(T)]_{min} = 1.0 \tag{5}$$

For class II events:

$$[m(T)]_{max} = 1.0 \tag{6}$$

$$[m(T)]_{min} = X_{max}(e^{x_{max}} - 1)^{-1} e^{0.5x_{max}} \tag{7}$$

where $X_{max} = \dfrac{\hbar \omega_{max,T,L}}{K_B T}$, $\hbar$ is the Planck constant divided by 2π, K_B is the Boltzmann constant, ω_{max} is the phonon frequency at the zone boundary of the first Brillouin zone, and suffixes T and L stand for transverse and longitudinal phonons, respectively. At the same time, he pointed out that the numerical value of $m(T)$ for class I events should not exceed 4 for transverse phonons and 3 for

longitudinal phonons. Thus, there still remains a large uncertainty in the assignment of an exact value of $m(T)$.

In the lack of an expression for the exact value of $m(T)$, to minimise the uncertainty, Dubey [33] suggested the use of the average value of its maximum and minimum values, which is more realistic compared to the use of the maximum value as suggested by Joshi and Verma [3]. Thus, the expression for $m(T)$ used by Dubey [33] can be expressed as

$$m_{\mathrm{I}}(T) = X_{\max}(e^{x\max} - 1)^{-1} + 0.5X_{\max} \tag{8}$$

for class I events, and

$$m_{\mathrm{II}}(T) = 0.5 + 0.5X_{\max}e^{0.5x\max}(e^{x\max} - 1)^{-1} \tag{9}$$

for class II events.

As stated earlier, the phonon-phonon scattering processes can be divided into two processes, N-processes and U-processes, and the scattering relaxation rates due to these processes are of the form [11–13]

$$\tau_{3\mathrm{ph,N}}^{-1} = B_{\mathrm{N}}g(\omega)T^{\mathrm{m(T)}} \tag{10}$$

for three-phonon N-processes [11] and

$$\tau_{3\mathrm{ph,U}}^{-1} = B_{\mathrm{U}}g(\omega)T^{\mathrm{m(T)}}e^{-\theta/\alpha T} \tag{11}$$

for three-phonon U-processes [12, 13], where B_{N} and B_{U} are the scattering strengths due to N and U-processes, respectively, θ is the Debye temperature of the sample, α is a constant, and suffixes N and U refer to N and U-processes, respectively. In view of Eqs (10) and (11), Dubey [33] expressed the scattering relaxation rates $\tau_{3\mathrm{ph,I}}^{-1}$ for class I events and $\tau_{3\mathrm{ph,II}}^{-1}$ for class II events as

$$\tau_{3\mathrm{ph,I}}^{-1} = (B_{\mathrm{N,I}} + B_{\mathrm{U,I}}e^{-\theta/\alpha T})g(\omega)T^{\mathrm{m_I(T)}} \tag{12}$$

$$\tau_{3\mathrm{ph,II}}^{-1} = (B_{\mathrm{N,II}} + B_{\mathrm{U,II}}e^{-\theta/\alpha T})g(\omega)T^{\mathrm{m_{II}(T)}} \tag{13}$$

Dubey [33] used the same frequency-dependence for N and U-processes due to the fact that the frequency-dependence $g(\omega)$ depends only on the polarisation branches. At the same time, the same value of $m(T)$ is assigned to both N and U-processes due to the fact that Guthrie [31] obtained the same value of $m(T)$ for both processes.

The Guthrie [31] classification of the phonon-phonon scattering events into class I and class II events leads to the participation of transverse phonons in class I events only, but the participation of longitudinal phonons in both class I and class II events. As a result, Dubey [33] proposed a new expression for $\tau_{3\mathrm{ph\,T}}^{-1}$, for transverse phonons

$$\tau_{3\mathrm{ph,T}}^{-1} = (B_{\mathrm{TN,I}} + B_{\mathrm{TU,I}}e^{-\theta/\alpha T})\omega T^{\mathrm{m_{T,I}(T)}} \tag{14}$$

because the contribution due to class II events is not possible for $\tau_{3ph,T}^{-1}$ for transverse phonons. Similarly, the expression for $\tau_{3ph,L}^{-1}$ for longitudinal phonons is given by [33]

$$\tau_{3ph,L}^{-1} = (B_{LN,I} + B_{LU,I}e^{-\theta/\alpha T})\omega^2 T^{mL,I(T)} + (B_{LN,II} + B_{LU,II}e^{-\theta/\alpha T})\omega^2 T^{mL,II(T)} \quad (15)$$

Besides the three-phonon scattering processes as discussed above, four-phonon scattering also plays an important role in the estimation of the lattice thermal conductivity at high temperatures. It was Pomeranchuk [34–36], first of all, who obtained a simple expression for the four-phonon scattering relaxation rate τ_{4ph}^{-1} as

$$\tau_{4ph}^{-1} = B_H \omega^2 T^2 \quad (16)$$

where B_H is the four-phonon scattering strength. The above expression for τ_{4ph}^{-1} has been used by a number of workers [3, 7, 10] to analyse the lattice thermal conductivities of different samples and it is found that it gives a good response to the experimental data.

The scattering of phonons due to point-defects, isotopes, etc. are most important scattering processes at temperatures near the conductivity maxima. At these temperatures, the high-frequency phonons are not excited to a large extent. When the wavelength of phonons is large compared to an imperfection in the crystal, the scattering can be treated in the manner of Lord Rayleigh [37]. Using the perturbation theory, Klemens [12] obtained an expression for the point-defect scattering relaxation rate τ_{pt}^{-1} for low-frequency phonons: this can be expressed as $\tau_{pt}^{-1} = A\omega^4$, where A is the point-defect scattering strength, given by

$$A = \frac{V}{4\pi v_s^3} \sum_i f_i \left(1 - \frac{m_i}{m}\right)^2 \quad (17)$$

where V is the atomic volume, f_i is the fraction of the i^{th} impure atom having mass m_i, m is the mass of the host lattice atom, and v_s is the average phonon velocity.

It is found [38–40] that the lattice thermal conductivity at lowest temperature can be explained very well on the basis of the boundary scattering alone. According to Casimir [38], the boundary scattering relaxation rate τ_B^{-1} can be expressed as $\tau_B^{-1} = v/L$, where v is the phonon velocity and L is the Casimir [38] length of the crystal, which depends on the size of the sample.

In view of the scattering relaxation rates stated above, the combined scattering relaxation rates $\tau_{c,T}^{-1}$ and $\tau_{c,L}^{-1}$ for transverse and longitudinal phonons, respectively, used in the present analysis are given by

$$\tau_{c,T}^{-1} = \tau_{B,T}^{-1} + A\omega^4 + (B_{TN,I} + B_{TU,I}e^{-\theta/\alpha T})\omega T^{mT,I(T)} + B_{HT}\omega^2 T^2 \quad (18)$$

$$\tau_{c,L}^{-1} = \tau_{B,L}^{-1} + A\omega^4 + (B_{LN,I} + B_{LU,I}e^{-\theta/\alpha T})\omega^2 T^{mL,I(T)} + (B_{LN,II} + B_{LU,II}e^{-\theta/\alpha T})\omega^2 T^{mL,II(T)} + B_{HL}\omega^2 T^2 \quad (19)$$

Assuming the spherical symmetry of the Brillouin zone (i.e. of the three polarization branches, one is longitudinal and two are transverse) and the fact that each phonon contributes separately towards the total lattice thermal conductivity, the contribution due to each mode of phonons can be expressed as

$$K_i = (1/6\pi^2) \int \tau_{c,i} v_{g,i}^2 (\hbar\omega/K_B T^2) e^{\hbar\omega/K_B T} (e^{\hbar\omega/K_B T} - 1)^{-2} q^2 dq + \Delta K \tag{20}$$

where integration is performed over the first Brillouin zone, v_g is the group velocity, q is the phonon wave vector, and suffix i stands for the polarisation branches. ΔK is the correction term [1] due to the three-phonon N-processes, and reduces to zero in the absence of the three-phonon normal processes. The correction term ΔK has been studied by several workers [41 – 50] and it is found that the contribution of ΔK towards the total lattice thermal conductivity is very small [42 – 50] at low and at high temperatures in the frame of the Callaway [1] integral as well as in the frame of the generalized Callaway integral [51, 52], its contribution can be ignored compared to the contribution due to the first term in eqn. (20). Solid He [41] and LiF [53], solid HD [54] are exceptions [41, 53, 54] to this.

Following the earlier work of Verma et al. [55], Dubey [33] used a better dispersion relation $q = (\omega/v)(1 + r\omega^2)$ to replace q into ω in eqn. (20), where r is a constant and depends on the dispersion curve of the sample under study. It can be calculated with the help of the experimental dispersion curve. It is needed to be stated that the velocity of phonons does not remain constant in the entire range of the first Brillouin zone. To be more exact, the entire first Brillouin zone can be divided into two ranges, $0 - \frac{1}{2} q_{max}$ and $\frac{1}{2} q_{max} - q_{max}$, where q_{max} is the phonon wave vector corresponding to the zone boundary of the first Brillouin zone, and following Verma et al. [55] different velocities are taken in the ranges $0 - \frac{1}{2} q_{max}$ and $\frac{1}{2} q_{max} - q_{max}$.

Thus, the total lattice thermal conductivity can be expressed as

$$K = K_T + K_L \tag{21}$$

where K_T and K_L are the contributions due to transverse and longitudinal phonons, respectively, and these are given by

$$K_T = \frac{C}{v_{T1}} \int_0^{\theta_1/T} \tau_{c,T} (1 + R_1 x^2 T^2)^2 (1 + 3R_1 x^2 T^2)^{-1} x^4 e^x (e^x - 1)^{-2} dx + \frac{C}{v_{T2}} \int_{\theta_1/T}^{\theta_2/T} \tau_{c,T} (1 + R_2 x^2 T^2)^2 (1 + 3R_2 x^2 T^2)^{-1} x^4 e^x (e^x - 1)^{-2} dx \tag{22}$$

$$K_L = \frac{C}{2v_{L1}} \int_0^{\theta_3/T} \tau_{c,L}(1 + R_3 x^2 T^2)^2 (1 + 3R_3 x^2 T^2)^{-1} x^4 e^x (e^x - 1)^{-2} dx$$

$$+ \frac{C}{2v_{L2}} \int_{\theta_3/T}^{\theta_4/T} \tau_{c,L}(1 + R_4 x^2 T^2)^2 (1 + 3R_3 x^2 T^2)^{-1} x^4 e^x (e^x - 1)^{-2} dx \quad (23)$$

where $C = (K_B/3\pi^2)(K_B T/\hbar)^3$, $R = r_i(K_B/\hbar)^2$, $i = 1, 2, 3$ and 4, $\tau_{c,i} = (\tau_{c,i}^{-1})^{-1}$, $i = T$ and L, $\theta_i = \hbar\omega_i/K_B$, $i = 1, 2, 3$ and 4, r_1 and r_2 are the dispersion constants for transverse phonons in the ranges $0 - \frac{1}{2}q_{max}$ and $\frac{1}{2}q_{max} - q_{max}$, respectively, r_3 and r_4 are the same for longitudinal phonons, v_{T1} and v_{T2} are the transverse phonon velocities in the ranges $0 - \frac{1}{2}q_{max}$ and $\frac{1}{2}q_{max} - q_{max}$, respectively, v_{L1} and v_{L2} are the same for longitudinal phonons, ω_1 and ω_2 are trans-

Table 3

The constants and parameters used in the calculation of the lattice thermal conductivities of Mg_2Si and Mg_2Ge in the temperature range 2 – 1000 K

Constants	Mg_2Si	Mg_2Ge
v_{T1} (cm/sec)	$4.6\ 10^5$	$3.9\ 10^5$
v_{T2} (cm/sec)	$1.4\ 10^5$	$1.8\ 10^5$
v_{L1} (cm/sec)	$6.4\ 10^5$	$5.8\ 10^5$
v_{L2} (cm/sec)	$5.1\ 10^5$	$2.4\ 10^5$
θ_1 (K)	154	140
θ_2 (K)	224	210
θ_3 (K)	254	306
θ_4 (K)	392	210
θ/α (K)	300	260
r_1 (sec^2)	$3.250\ 10^{-28}$	$1.24\ 10^{-28}$
r_2 (sec^2)	$6.428\ 10^{-28}$	$5.534\ 10^{-28}$
r_3 (sec^2)	$1.019\ 10^{-29}$	$2.66\ 10^{-28}$
r_4 (sec^2)	$8.804\ 10^{-29}$	$6.518\ 10^{-29}$
τ_{BT}^{-1} (sec^{-1})	$5.68\ 10^6$	$1.7\ 10^6$
τ_{BL}^{-1} (sec^{-1})	$7.90\ 10^6$	$2.6\ 10^6$
A (sec^3)	$8.0\ 10^{-46}$	$1.4\ 10^{-44}$
$B_{TN,I}$ (deg^{-m})	$1.7\ 10^{-12}$	$1.0\ 10^{-12}$
$B_{TU,I}$ (deg^{-m})	$4.61\ 10^{-5}$	$3.6\ 10^{-5}$
$B_{LN,I}$ (sec. deg^{-m})	$5.0\ 10^{-24}$	$1.0\ 10^{-24}$
$B_{LU,I}$ (sec. deg^{-m})	$1.0\ 10^{-22}$	$1.0\ 10^{-23}$
$B_{LN,II}$ (sec. deg^{-m})	$5.25\ 10^{-20}$	$1.0\ 10^{-22}$
$B_{LU,II}$ (sec. deg^{-m})	$7.0\ 10^{-17}$	$3.0\ 10^{-17}$
B_{HT} (sec. deg^{-2})	$1.2\ 10^{-23}$	$1.0\ 10^{-24}$
B_{HL} (sec. deg^{-2})	$1.2\ 10^{-23}$	$1.0\ 10^{-24}$

verse phonon frequencies corresponding to the wave vectors $\frac{1}{2}q_{max}$ and q_{max}, respectively, ω_3 and ω_4 are the same for longitudinal phonons, and $\tau_{c,T}^{-1}$ and $\tau_{c,L}^{-1}$ are the combined scattering relaxation rates for transverse and longitudinal phonons, respectively, as stated earlier.

Lattice thermal conductivity of Mg_2Ge

The constants relating to the dispersion curve are calculated with the help o- the experimental dispersion curve of Mg_2Ge reported by Chung et al. [56], anp the values obtained are reported in Table 3. Using these constants, the tempera ture exponents $m_{T,I}(T)$ for class I events for transverse phonons and $m_{L,I}(T)$ and $m_{L,II}(T)$ for longitudinal phonons for class I and class II events, respectively, fio the three-phonon scattering relaxation rates have been calculated for Mg_2Ge fn

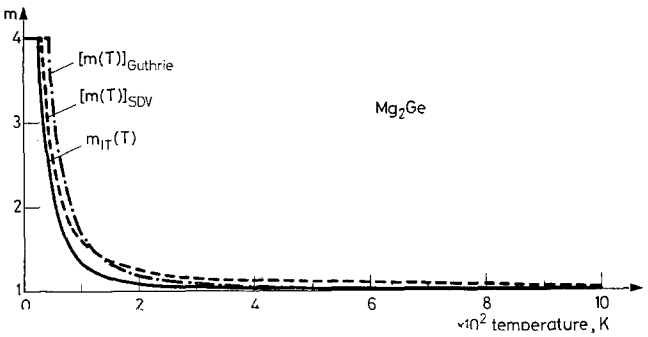

Fig. 1. The temperature exponent $m_{T,I}(T)$ for class I events for transverse phonons for Mg_2Ge. Solid line represents values of $m_{T,I}(T)$ used in the present analysis. Dashed line represents values obtained in the frame of the SDV model, while dot-dashed line shows the upper limit of Guthrie

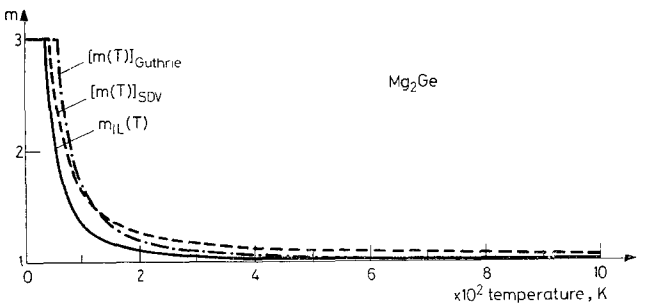

Fig. 2. The temperature exponent $m_{L,I}(T)$ for class I events for longitudinal phonons for Mg_2Ge. Solid line represents values of $m_{L,I}(T)$ used in the present analysis. Dashed line represents values obtained in the frame of the SDV model, while dot-dashed line shows the upper limit of Guthrie

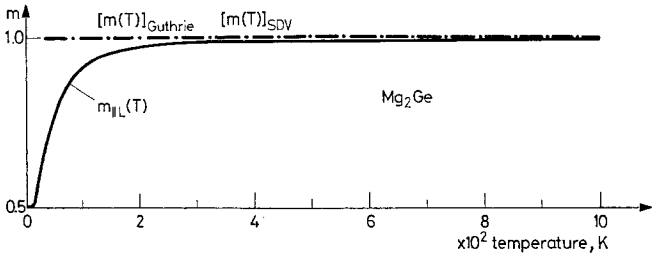

Fig. 3. The temperature exponent $m_{L,II}(T)$ for class II events for longitudinal phonons for Mg_2Ge. Solid line represents values of $m_{L,II}(T)$ used in the present analysis. Dot-dashed lines shows the value used in the SDV model as well as the upper limit of Guthrie

the entire temperature range 2–1000 K with the help of eqns. (8) and (9); the results obtained are reported in Figs 1–3. To make them more clear, these values are also listed in Table 4. To have a comparative study of the temperature expo-

Table 4

The temperature exponents $m_{T,I}(T)$, $m_{L,I}(T)$ and $m_{L,II}(T)$ for τ_{3ph}^{-1} for Mg_2Ge in the temperature range 2–1000 K. $m_{T,I}(T)$ for class I events for transverse phonons, $m_{L,I}(T)$ and $m_{L,II}(T)$ for class I and class II events, respectively, for longitudinal phonons

T, K	$m_{T,I}(T)$	$m_{L,I}(T)$	$m_{L,II}(T)$
1000	1.00367	1.00367	0.99908
900	1.00453	1.00453	0.99886
800	1.00573	1.00573	0.99856
700	1.00748	1.00748	0.99812
600	1.01018	1.01018	0.99745
500	1.01465	1.01465	0.99634
400	1.02266	1.02286	0.99430
300	1.04050	1.04050	0.98993
200	1.09022	1.09022	0.99774
100	1.34304	1.34304	0.91870
90	1.41723	1.41723	0.90231
80	1.51750	1.51750	0.88084
70	1.65718	1.65718	0.85223
60	1.85898	1.85898	0.81357
50	2.16394	2.16394	0.76107
40	2.65269	2.65269	0.69115
30	3.50638	3.0	0.60578
20	4.0	3.0	0.52755
10	4.0	3.0	0.50028
8	4.0	3.0	0.50002
6	4.0	3.0	0.5
4	4.0	3.0	0.5
2	4.0	3.0	0.5

nents used in the present analysis with those of the earlier workers, the temperature exponents have been calculated in the frame of the Sharma – Dubey – Verma (SDV) model [4, 5], and the results obtained are reported in Figs 1 – 3, together with $m(T)$ used in the present analysis. The upper limits of $m(T)$ found by Guthrie [31] have been calculated in the entire temperature range of study, and the results obtained are shown in Figs 1 – 3.

Following the work of the earlier workers, and considering that at lowest temperature the entire lattice thermal resistivity of the sample under study is due

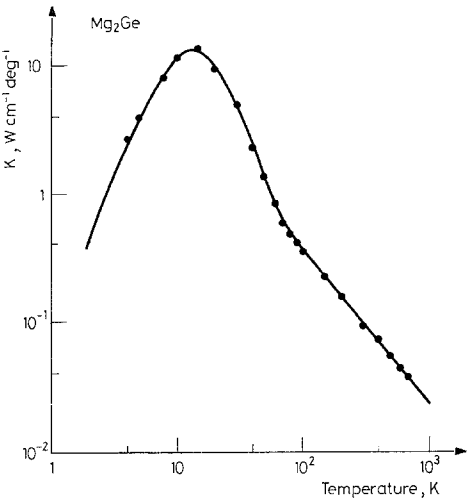

Fig. 4. Total lattice thermal conductivity of Mg_2Ge in the temperature range 2– 1000 K. Solid line shows calculated values, and circles are experimental points

mainly to boundary scattering, the Casimir length [38] of the sample has been calculated at 2 K; hence, the boundary scattering relaxation rates $\tau_{B,T}^{-1}$ and $\tau_{B,L}^{-1}$ for transverse and longitudinal phonons, respectively, are calculated at 2 K. The values of these two constants are found to be the same as obtained by Dubey [57, 58]. The point-defect scattering strength A has been adjusted at 8 K, ignoring the contribution due to the three-phonon scattering relaxation rate. The value obtained is the same as reported by Dubey [58, 59] and by Martin [59].

As we know, at low temperatures $\tau_{3ph,N}^{-1}$ dominates over $\tau_{3ph,U}^{-1}$, while $\tau_{3ph,U}^{-1}$ dominates over $\tau_{3ph,N}^{-1}$ at high temperatures. Following the earlier work of Dubey [33] and considering the fact stated above, approximate values of constants $B_{TN,I}$, $B_{LN,I}$ and $B_{LN,II}$ have been calculated at 20 K, ignoring the contribution due to $\tau_{3ph,U}^{-1}$, with the help of the experimental values of the lattice thermal conductivity, while the approximate values of the constants $B_{TU,I}$, $B_{LU,I}$ and $B_{LU,II}$ are estimated at 200 K, neglecting the contribution due to $\tau_{3ph,N}^{-1}$. The values of these constants have been further corrected at 100 K, considering the contributions

of $\tau_{3ph,N}^{-1}$ and of $\tau_{3ph,U}^{-1}$. The constants B_{HT} and B_{HL} related to the four-phonon scattering strength are calculated at 500 K with the help of the numerical integration of the conductivity integrals. The values of these constants, as obtained above, are listed in Table 3. The experimental data on the lattice thermal conductivity of Mg_2Ge for the theoretical verification are taken from the earlier report of Martin [59].

Using the constants reported in Table 3, the total lattice thermal conductivity of Mg_2Ge has been calculated in the entire temperature range 2–1000 K by

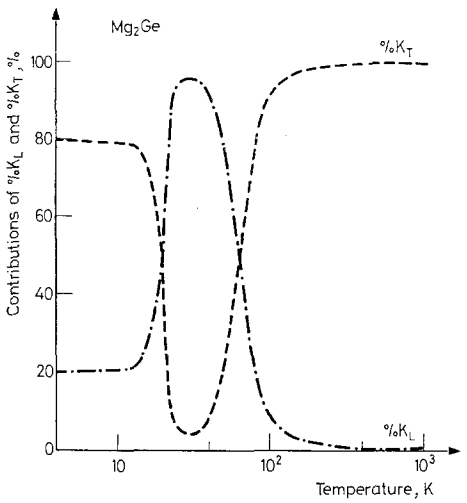

Fig. 5. The percentage contributions % K_T and % K_L towards the total lattice thermal conductivity of Mg_2Ge due to transverse and longitudinal phonons, respectively. Dashed and dot-dashed lines represent % K_T and % K_L, respectively

estimating the separate contributions K_T due to transverse, and K_L due to longitudinal phonons, with the help of the numerical integration of the conductivity integrals in eqns. (22) and (23), respectively, and the results obtained are shown in Fig. 4. The separate percentage contribution % K_T and % K_L due to transverse and longitudinal phonons, respectively, towards the total lattice thermal conductivity have been analysed in the entire temperature range 2–1000 K, and the results obtained are reported in Fig. 5.

To analyse the roles of three-phonon N- and U-processes, the percentage contributions of $\tau_{3ph,N}^{-1}$ and $\tau_{3ph,U}^{-1}$ towards the three-phonon scattering relaxation rate τ_{3ph}^{-1} have been studied for class I events for transverse phonons, and for class I and class II events for longitudinal phonons for Mg_2Ge in the entire temperature range 2–1000 K, and the results obtained are illustrated in Figs 6–8. The percentage contributions of $\tau_{3ph,T}^{-1}$ for class I events for transverse phonons, and $\tau_{3ph,L}^{-1}$ (class I + class II) for longitudinal phonons, towards the combined

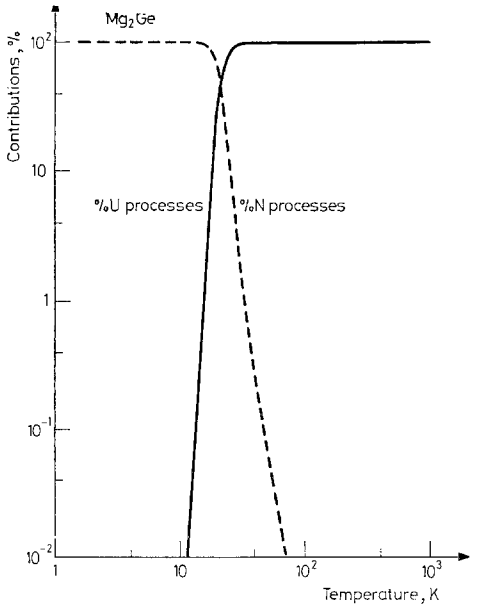

Fig. 6. The percentage contributions $\%\,\tau_{3ph,N}^{-1}$ and $\%\,\tau_{3ph,U}^{-1}$ processes towards the $\tau_{3ph,T}^{-1}$ for class I events for transverse phonons for Mg_2Ge in the temperature range 2–1000 K. Solid and dashed lines represent $\%\,\tau_{3ph,U}^{-1}$ and $\%\,\tau_{3ph,N}^{-1}$, respectively

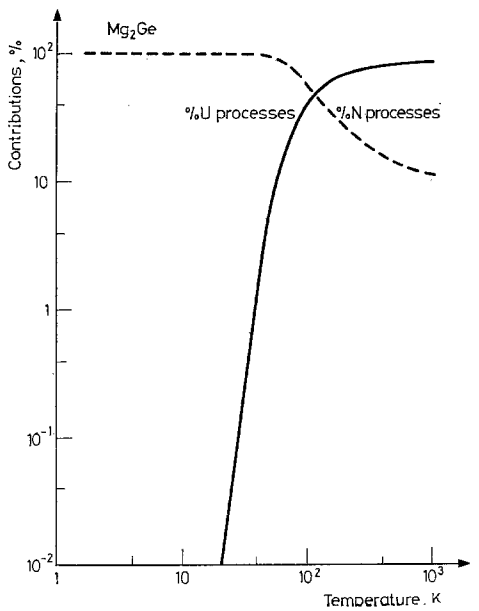

Fig. 7. The percentage contributions $\%\,\tau_{3ph,N}^{-1}$ and $\%\,\tau_{3ph,U}^{-1}$ towards $\tau_{3ph,L}^{-1}$ for class I event for longitudinal phonons for Mg_2Ge in the temperature range 2–1000 K. Solid and dashed lines represent $\%\,\tau_{3ph,U}^{-1}$ and $\%\,\tau_{3ph,N}^{-1}$, respectively

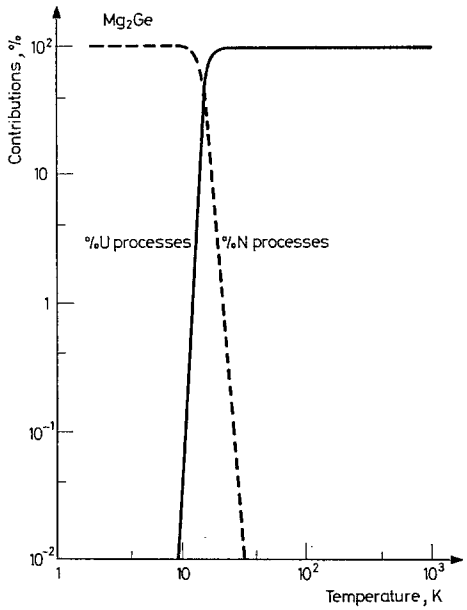

Fig. 8. The percentage contributions $\%\,\tau_{3ph,N}^{-1}$ and $\%\,\tau_{3ph,U}^{-1}$ towards $\tau_{3ph,L}^{-1}$ for class II events for Mg_2Ge in the temperature range 2—1000 K. Solid and dashed lines represent $\%\,\tau_{3ph,U}^{-1}$ and $\%\,\tau_{3ph,N}^{-1}$, respectively

scattering relaxation rates of the respective modes $\tau_{c,T}^{-1}$ and $\tau_{c,L}^{-1}$ are calculated for the four different values of the phonon frequency $\omega = \frac{1}{4}\omega_{max}, \frac{1}{2}\omega_{max}\frac{3}{4}\omega_{max}$ and ω_{max}, in the absence of the four-phonon scattering processes; the results obtained are reported in Tables 5 and 6.

Lattice thermal conductivity of Mg_2Si

The experimental data on the lattice thermal conductivity of Mg_2Si for the theoretical analysis are taken from the earlier report of Martin [59]. The constants relating to the dispersion curve are calculated with the help of the experimental dispersion curve reported by Whitten et al. [60], and the values obtained are listed in Table 3. Using these constants, the temperature exponents $m_{T,I}(T)$ for class I events for transverse phonons, and $m_{L,I}(T)$ and $m_{L,II}(T)$ for class I and class II events, respectively, for longitudinal phonons, have been calculated with the help of Eqs (8) and (9) similarly as for Mg_2Ge, in the entire temperature range 2—1000 K, and the results obtained are listed in Table 7. The values of $m(T)$ used in the SDV model [4, 5] and the upper limits of Guthrie [31] have also been estimated, and the results are shown in Figs 9—11, together with $m(T)$ used in the present analysis.

Table 5

The percentage contribution of the three-phonon scattering relaxation rate $\tau_{3ph,T}^{-1}$ towards the combined scattering relaxation rate $\tau_{c,T}^{-1}$ due to transverse phonons for Mg_2Ge due to class I events in the absence of the four-phonon processes for four different values of the phonon frequencies. ω_{max} represents the maximum frequency of transverse phonons

T, K	$\%\,\tau_{3ph,T}^{-1}$ for $\omega = \frac{1}{4}\omega_{max}$	$\%\,\tau_{3ph,T}^{-1}$ for $\omega = \frac{1}{2}\omega_{max}$	$\%\,\tau_{3ph,T}^{-1}$ for $\omega = \frac{3}{4}\omega_{max}$	$\%\,\tau_{3ph,T}^{-1}$ for $\omega = \omega_{max}$
1000	99.98	99.87	99.57	98.98
900	99.98	99.85	99.51	98.85
800	99.97	99.83	99.43	98.67
700	99.97	99.80	99.33	98.43
600	99.96	99.75	99.18	98.09
500	99.95	99.68	98.96	97.57
400	99.94	99.57	98.59	96.73
300	99.91	99.36	97.89	95.15
200	99.84	98.86	96.26	91.58
100	99.63	97.26	91.35	81.68
90	99.59	96.99	90.56	80.19
80	99.55	96.72	89.77	78.75
70	99.52	96.48	89.08	77.49
60	99.50	96.31	88.60	76.64
50	99.49	96.27	88.47	76.41
40	99.50	96.34	88.67	76.37
30	99.49	96.25	88.41	76.30
20	73.39	26.53	9.69	4.33
10	0.20	0.02	0.01	0
8	0.08	0.01	0	0
6	0.02	0	0	0
4	0	0	0	0
2	0	0	0	0

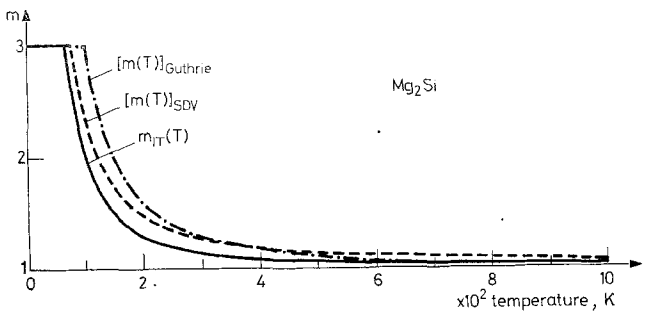

Fig. 9. The temperature exponent $m_{T,I}(T)$ for class I events for transverse phonons for Mg_2Si. Solid line represents values of $m_{T,I}(T)$ used in the present analysis. Dashed line represents values obtained in the frame of the SDV model, while dot-dashed line shows the upper limit of Guthrie

Table 6

The percentage contribution of the three-phonon scattering relaxation rate $\tau_{3ph,L}^{-1}$ towards the combined scattering relaxation rate $\tau_{c,L}^{-1}$ for Mg_2Ge due to the combined effect of class I and class II events in the absence of four-phonon processes for four different values of the phonon frequency. ω_{max} represents the maximum frequency of longitudinal phonons

T, K	$\%\,\tau_{3ph,L}^{-1}$ for $\omega = \frac{1}{4}\omega_{max}$	$\%\,\tau_{3ph,L}^{-1}$ for $\omega = \frac{1}{2}\omega_{max}$	$\%\,\tau_{3ph,L}^{-1}$ for $\omega = \frac{3}{4}\omega_{max}$	$\%\,\tau_{3ph,L}^{-1}$ for $\omega = \omega_{max}$
1000	100	99.98	99.97	99.95
900	100	99.98	99.97	99.95
800	100	99.98	99.96	99.94
700	100	99.98	99.96	99.93
600	100	99.97	99.95	99.91
500	100	99.96	99.93	99.88
400	99.98	99.95	99.90	99.83
300	99.98	99.92	99.83	99.70
200	99.95	99.81	99.59	99.28
100	99.54	98.29	96.26	93.54
90	99.27	97.32	94.20	90.14
80	98.74	95.41	90.26	83.91
70	97.48	91.14	82.10	72.08
60	93.99	80.51	64.90	51.00
50	82.23	55.07	35.35	23.53
40	45.88	18.34	9.10	5.34
30	8.85	2.51	1.13	0.64
20	1.23	0.33	0.15	0.08
10	0.18	0.05	0.022	0.01
8	0.11	0.03	0.01	0
6	0.06	0.02	0	0
4	0.04	0	0	0
2	0.02	0	0	0

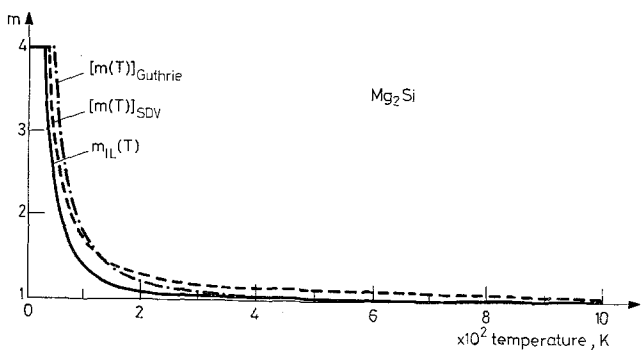

Fig. 10. The temperature exponent $m_{L,I}(T)$ for class I events for longitudinal phonons fo Mg_2Si. Solid line represents values of $m_{L,I}(T)$ used in the present analysis. Dashed line represents values obtained in the frame of the SDV model, while dot-dashed line shows the upper limit of Guthrie

Table 7

The temperature exponents $m_{T,I}(T)$, $m_{L,I}(T)$ and $m_{L,II}(T)$ for τ_{3ph}^{-1} for Mg_2Si in the temperature range 2—1000 K. $m_{T,I}(T)$ for class I events for transverse phonons, $m_{L,I}(T)$ and $m_{L,II}(T)$ for class I and class II events, respectively, for longitudinal phonons

T, K	$m_{T,I}(T)$	$m_{L,I}(T)$	$m_{L,II}(T)$
1000	1.00417	1.01277	0.99681
900	1.00515	1.01575	0.99606
800	1.00652	1.01992	0.99503
700	1.00851	1.02599	0.99352
600	1.01158	1.03531	0.99121
500	1.01666	1.05070	0.98742
400	1.02599	1.07878	0.98053
300	1.04603	1.13839	0.96612
200	1.10241	1.30134	0.82810
100	1.38687	2.03935	0.78167
90	1.46972	2.23440	0.74993
80	1.58129	2.48676	0.71360
70	1.73598	2.82078	0.67090
60	1.95812	3.0	0.62475
50	2.29135	3.0	0.57780
40	2.82078	3.0	0.53641
30	2.73760	3.0	0.50950
20	4.0	3.0	0.50054
10	4.0	3.0	0.5
8	4.0	3.0	0.5
6	4.0	3.0	0.5
4	4.0	3.0	0.5
2	4.0	3.0	0.5

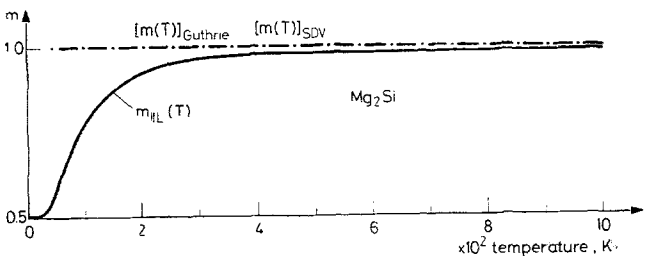

Fig. 11. The temperature exponent $m_{L,II}(T)$ for class II events for longitudinal phonons for Mg_2Si. Solid line represents values of $m_{L,II}(T)$ used in the present analysis. Dot-dashed line shows values used in the SDV model as well as the upper limit of Guthrie

The boundary scattering relaxation rates $\tau_{B,T}^{-1}$ and $\tau_{B,L}^{-1}$ for transverse and longitudinal phonons, respectively, and the point-defect scattering strength A have been calculated at 2 and 8 K, respectively, similarly as for Mg_2Ge, and the values obtained are the same as obtained by Dubey [58, 61]. The constants relating to three-phonon and four-phonon scattering strengths have been estimated at different temperatures as stated in the earlier section for Mg_2Ge, and the values obtained are listed in Table 3.

Using the constants reported in Table 3, the total lattice thermal conductivity of Mg_2Si has been calculated in the entire temperature range 2–1000 K by estimating the contributions K_T and K_L separately with the help of the numerical

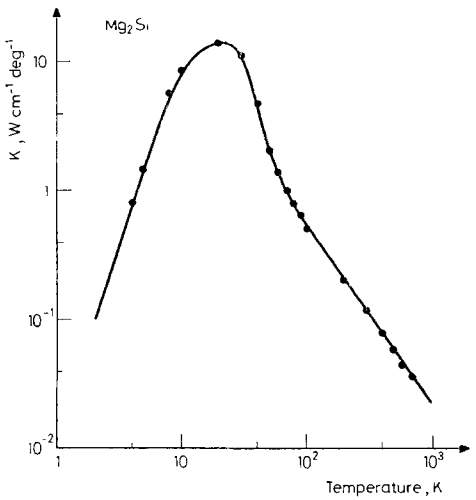

Fig. 12. Total lattice thermal conductivity of Mg_2Si in the temperature range 2–1000 K. Solid line shows calculated values, and circles are experimental points

integration of eqns. (22) and (23), and the results obtained are shown in Fig. 12. To study the relative contribution of each mode, the percentage contributions $\%\, K_T$ and $\%\, K_L$ towards the total lattice thermal conductivity of Mg_2Si have been analysed in the temperature range 2–1000 K, and the results obtained are illustrated in Fig. 13.

To study the relative roles of three-phonon N and U-processes, the percentage contributions $\%\, \tau_{3ph,N}^{-1}$ and $\%\, \tau_{3ph,U}^{-1}$ towards the three-phonon scattering relaxation rate τ_{3ph}^{-1} have been analysed for class I events for transverse phonons and class I and class II events for longitudinal phonons, similarly as for Mg_2Ge, and the results obtained are shown in Figs 14–16. To see the importance of τ_{3ph}^{-1} in the estimation of the lattice thermal conductivity, the percentage contributions of $\tau_{3ph,T}^{-1}$ of class I events for transverse phonons and $\tau_{3ph,L}^{-1}$ (class I + class II) for longitudinal phonons towards the combined scattering relaxation rates $\tau_{c,T}^{-1}$

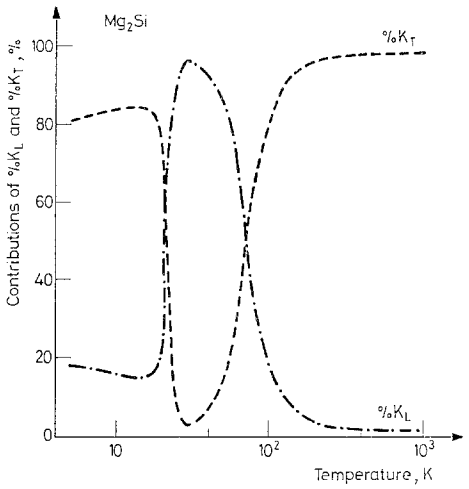

Fig. 13. The percentage contributions $\%\ K_T$ and $\%\ K_L$ towards the total lattice thermal conductivity of Mg_2Si due to transverse and longitudinal phonons, respectively. Dashed and dot-dashed line represent $\%\ K_T$ and $\%\ K_L$, respectively

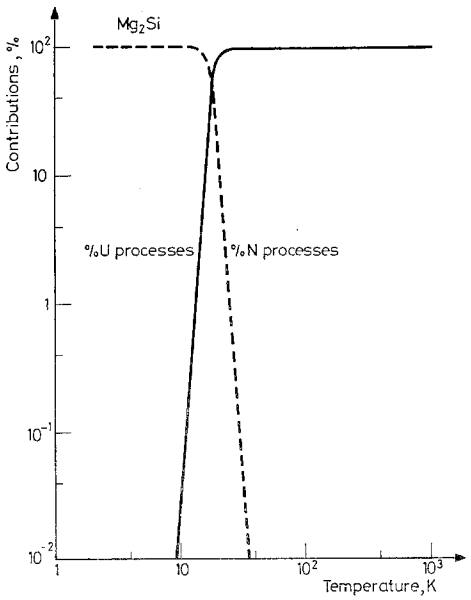

Fig. 14. The percentage contributions $\%\ \tau^{-1}_{3ph,N}$ and $\%\ \tau^{-1}_{3ph,U}$ towards $\tau^{-1}_{3ph,T}$ for class I events for transverse phonons for Mg_2Si in the temperature range 2 – 1000 K. Solid and dashed lines represent $\%\ \tau^{-1}_{3ph,U}$ and $\%\ \tau^{-1}_{3ph,N}$, respectively

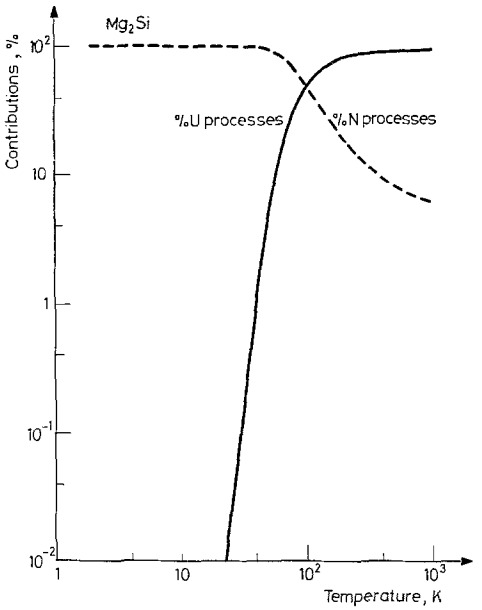

Fig. 15. The percentage contributions % $\tau_{3ph,N}^{-1}$ and % $\tau_{3ph,U}^{-1}$ towards $\tau_{3ph,L}^{-1}$ for class I event for longitudinal phonons for Mg_2Si in the temperature range 2—1000 K. Solid and dashed lines represent % $\tau_{3ph,U}^{-1}$ and $\tau_{3ph,N}^{-1}$, respectively

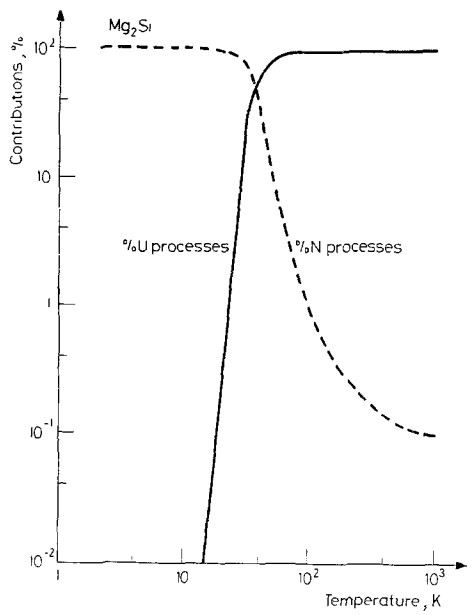

Fig. 16. The percentage contributions % $\tau_{3ph,N}^{-1}$ and % $\tau_{3ph,U}^{-1}$ towards $\tau_{3ph,L}^{-1}$ for class II events for Mg_2Si in the temperature range 2—1000 K. Solid and dashed lines represent % $\tau_{3ph,U}^{-1}$ and % $\tau_{9ph,N}^{-1}$, respectively

Table 8

The percentage contribution of the three-phonon scattering relaxation rate $\tau_{3ph,T}^{-1}$ towards the combined scattering relaxation rate $\tau_{c,T}^{-1}$ due to transverse phonons for Mg_2Si due to class I events in the absence of four-phonon processes for four different values of the phonon frequency. ω_{max} represents the maximum frequency of transverse phonons

T, K	$\%\,\tau_{3ph,T}^{-1}$ for $\omega = \frac{1}{4}\omega_{max}$	$\%\,\tau_{3ph,T}^{-1}$ for $\omega = \frac{1}{2}\omega_{max}$	$\%\,\tau_{3ph,T}^{-1}$ for $\omega = \frac{3}{4}\omega_{max}$	$\%\,\tau_{3ph,T}^{-1}$ for $\omega = \omega_{max}$
1000	100	100	99.97	99.94
900	100	100	99.97	99.93
800	100	99.98	99.96	99.92
700	100	99.98	99.96	99.90
600	100	99.98	99.95	99.88
500	100	99.97	99.93	99.85
400	99.98	99.97	99.91	99.80
300	99.98	99.95	99.86	99.69
200	99.96	99.91	99.75	99.42
100	99.92	99.78	99.36	98.52
90	99.91	99.76	99.28	98.36
80	99.90	99.73	99.21	98.19
70	99.89	99.71	99.14	98.02
60	99.88	99.69	99.07	97.88
50	99.87	99.67	99.02	97.77
40	99.87	99.65	98.96	97.63
30	99.84	99.58	98.75	97.15
20	69.87	46.49	22.37	11.04
10	1.53	0.58	0.19	0.08
8	0.63	0.23	0.07	0.03
6	0.20	0.07	0.02	0.01
4	0.03	0.01	0	9
2	0	0	0	0

and $\tau_{c,L}^{-1}$ of the respective modes have been studied for the four different values of the phonon frequency $\omega = \frac{1}{4}\omega_{max}, \frac{1}{2}\omega_{max}, \frac{3}{4}\omega_{max}$ and ω_{max} in the absence of four-phonon processes; the results obtained are listed in Tables 8 and 9.

Comparative investigation of the present study with the previous study

To see the value of the present study, it is needed to make a comparative study of the present analysis with the previous studies, and the present section is concerned with this. Martin [59] studied the lattice thermal conductivities of Mg_2Ge and Mg_2Si in the temperature range 4–700 K in the frame of the two-mode conduction of phonons proposed by Holland [2]. From Tables 1 and 2, it is clear that

Table 9

The percentage contribution of the three-phonon scattering rate $\tau_{3ph,L}^{-1}$ towards the combined scattering relaxation rate $\tau_{c,L}^{-1}$ for Mg_2Si due to longitudinal phonons due to the combined effect of class I and class II events in the absence of four-phonon processes for four different values of the phonon frequency. ω_{max} represents the maximum frequency of longitudinal phonons

T, K	$\%\,\tau_{3ph,L}^{-1}$ for $\omega = \frac{1}{4}\omega_{max}$	$\%\,\tau_{3ph,L}^{-1}$ for $\omega = \frac{1}{2}\omega_{max}$	$\%\,\tau_{3ph,L}^{-1}$ for $\omega = \frac{3}{4}\omega_{max}$	$\%\,\tau_{3ph,L}^{-1}$ for $\omega = \omega_{max}$
1000	100	100	100	100
900	100	100	100	100
800	100	100	100	100
700	100	100	100	100
600	100	100	100	100
500	100	100	100	99.98
400	100	100	99.98	99.98
300	100	100	99.98	99.96
200	100	99.97	99.94	99.90
100	99.86	99.58	99.08	98.39
90	99.75	99.28	98.43	97.25
80	99.54	98.63	97.04	94.87
70	99.04	97.18	93.98	89.80
60	97.80	93.68	87.03	79.11
50	94.01	83.97	70.33	57.22
40	84.55	64.611	45.24	31.79
30	71.46	45.51	27.43	17.58
20	60.50	33.81	18.78	11.54
10	48.76	24.09	12.56	7.49
8	45.67	21.89	11.25	6.68
6	41.91	19.40	9.82	5.79
4	36.95	16.35	8.12	4.75
2	29.25	12.11	5.87	3.40

(in the frame of the Holland model) Martin [59] could not consider the contribution of three-phonon N-processes in the range $\frac{1}{2}q_{max} - q_{max}$ and three-phonon U-processes in the range $0 - \frac{1}{2}q_{max}$ in the calculation of the lattice thermal conductivity K_T due to transverse phonons. At the same time, it is also clear that he could not consider the contribution of the three-phonon U-processes in the entire range of the Brillouin zone $0 - q_{max}$ in the calculation of the lattice thermal conductivity K_L due to longitudinal phonons. Thus, it can be said that Martin [59] used only one process (either N- or U-process) in the calculation of the lattice thermal conductivities of Mg_2Ge and Mg_2Si. From Tables 1 and 2, it is also clear that (in the frame of the Holland [2] model) Martin [59] used the Herring [11]

relations $\tau_{3ph,T}^{-1} \propto \omega T^4$ and $\tau_{3ph,L}^{-1} \propto \omega v T^3$ for three-phonon N-processes in the entire temperature range of study, which are valid at low temperatures only.

Misho and Dubey [62] calculated the lattice thermal conductivities of Mg_2Ge and Mg_2Si in the temperature range 4 – 1000 K in the frame of the expression for τ_{3ph}^{-1} proposed by Joshi and Verma [3]. From Tables 1 and 2, it is clear that (in the frame of Joshi and Verma [3]) they could not consider the contribution of three-phonon U-processes. At the same time, they used discrete values of the temperature exponent $m(T)$ in place of a continuous value. However, they tried to use the Guthrie [31] expression for the temperature exponent $m(T)$.

The lattice thermal conductivities of Mg_2Ge and Mg_2Si were studied by Dubey [57, 58] in the temperature range 4 – 800 K in the frame of the Sharma – Dubey – Verma (SDV) model [4, 5]. From Tables 1 and 2, it is clear that Dubey [58, 59] (in the frame of the SDV model [4, 5]) ignored the contribution of the three-phonon N-processes in the calculation of the lattice thermal conductivity in the entire temperature range. At the same time the expression (see Eqs 5, 6 and 22 of ref. 4) for the temperature exponent $m(T)$ used in the SDV model [4, 5] contains an empirical factor $(1 + \theta/\alpha T)$. However, it must be stated that Dubey [57, 58] was the first to use a continuous value of the temperature exponent $m(T)$ in the analysis of the lattice thermal conductivities of MgGe and of Mg_2Si.

With the help of Eqs (8) and (9), it is clear that in the present analysis of the lattice thermal conductivities of Mg_2Ge and Mg_2Si, the Guthrie [31] expression for the temperature exponent $m(T)$ for τ_{3ph}^{-1} has been incorporated without any empirical factor. At the same time, the contributions due to three-phonon N and U-processes are included in the entire temperature range 2 – 1000 K for transverse and longitudinal phonons. The expression for τ_{3ph}^{-1} used in the present analysis is based on the Guthrie [31] classification of class I and class II events. At the same time, it is also based on the N- and U-processes. The role of the four-phonon processes is included in the present study. It is interesting to note that the role of the three-phonon scattering relaxation rate has been reported in more detail in the present work.

Results and discussion

First of all, we shall discuss the three-phonon scattering relaxation rate and its temperature exponents. The temperature exponents $m_{T,I}(T)$, $m_{L,I}(T)$ and $m_{L,II}(T)$ used in the present analysis can be studied with the help of Tables 4 and 7 for Mg_2Ge and Mg_2Si, respectively, while their continuous nature can be seen with the help of Figs 1 – 3 and Figs 9 – 11 for Mg_2Ge and Mg_2Si, respectively. With the help of these Tables and Figures, it can be seen that at high temperatures $m_{T,I}(T)$, $m_{L,I}(T)$ and $m_{L,II}(T)$ tend to unity. As a result, at high temperatures ($e^{-\theta/\alpha T} \rightarrow 1$ due to the large value of T) the expression used for τ_{3ph}^{-1} reduces to $\tau_{3ph}^{-1} \propto T$, which is similar to the earlier findings of Herring [11]. At the same time, it also results in $K \propto 1/T$ at high temperatures, which is similar to the previous findings. At low temperatures, $m_{T,I}(T)$ and $m_{L,I}(T)$ tend to 4 and 3, respec-

tively, which are the same as reported by Herring [11]. Through the numerical analysis of the conductivity integrals for K_L, it is found that at low temperatures the scattering relaxation rate due to class II events is much smaller compared to the same due to class I events. At the same time, due to the low value of T, the factor $e^{-\theta/\alpha T}$ is negligibly small. Thus, the expression for τ_{3ph}^{-1} used in the present analysis reduces to $\tau_{3ph}^{-1} \propto \omega T^4$ for transverse phonons and $\tau_{3ph}^{-1} \propto \omega 2T^3$ for longitudinal phonons, which are similar to the earlier findings of Herring [11]. From these Figures, it is also clear that the values of $m(T)$ used in the calculation of the lattice thermal conductivities of Mg_2Ge and Mg_2Si lie in the range $1-4$ for transverse phonons and $1-3$ for longitudinal phonons in the entire temperature range $2-1000$ K, and the upper limit of Guthrie [31] is not exceeded at any temperature. Thus, they are free from the Guthrie comments [32] too. Therefore, it can be said that the values of $m(T)$ used in the present analysis of the lattice thermal conductivities of Mg_2Ge and Mg_2Si are more realistic than those used by earlier workers [57, 58, 61, 62].

With the help of Figs 4 and 12, it can be seen that the agreement between the calculated and experimental values of the lattice thermal conductivity is very good in the entire temperature range $2-1000\ \Theta$ for both Mg_2Ge and Mg_2Si. Thus, one can say that the expression used for τ_{3ph}^{-1} gives a good response to the experimental data on the lattice thermal conductivity at low and at high temperatures. In other words, it can be said that the experimental data on the lattice thermal conductivity of a sample can be explained well in the frame of the expression for τ_{3ph}^{-1} proposed by Dubey [33].

The relative contributions of transverse and longitudinal phonons towards the total lattice thermal conductivities of Mg_2Ge and Mg_2Si can be studied with the help of Figs 5 and 13, respectively. From these two Figures, it can be seen that at high temperatures the percentage contribution $\%\, K_T$ due to transverse phonons dominates over $\%\, K_L$. In other words, one can say that at high temperature most of the heat is carried by transverse phonons, which is similar to the findings of the previous workers [2–7, 63–65] based on the relaxation time approach [2–7] and on the variational method [63–65]. From these two Figures, it is clear that at low temperatures $\%\, K_T$ is larger than $\%\, K_L$, which can be understood as follows. At very low temperatures, the lattice thermal resistivity is mainly due to the boundary scattering and the lattice specific heat $\propto T^3$. As a result, the ratio $\%\, K_T / \%\, K_L$ depends upon the factor

$$2(v_L\, \tau_{B,L}^{-1} / v_T\, \tau_{B,T}^{-1}) = 2(v_L/v_T)^2 .$$

Thus, the percentage contribution $\%\, K_T$ due to transverse phonons dominates over $\%\, K_L$ at low temperature too, which is similar to the results reported by previous workers [55]. At a little higher temperature towards the conductivity maxima, $\%\, K_T$ begins to decrease with increasing temperature and, after attaining a minimum value (say 3.2 for Mg_2Ge and 3.5 for Mg_2Si), at a certain temperature (say 30 K for Mg_2Ge and 30 K for Mg_2Si) it begins to increase again. The

reverse nature is also true for longitudinal phonons. The nature of such variation can be explained by considering the role of the point-defect scattering (see ref. 55). These results are similar to those obtained by Sharma et al. [55], for Ge on the basis of the Holland [2] model. At the same time, it is also similar to those obtained by Dubey [58] for Mg_2Ge in the frame of the SDV model [4, 5].

The relative importance of three-phonon N- and U-processes in the calculation of the lattice thermal conductivities of Mg_2Ge and Mg_2Si can be studied with the help of Figs 6–8 and 14–16, respectively. From these Figures, it is clear that at low temperature $\tau_{3ph,N}^{-1}$ dominates over $\tau_{3ph,U}^{-1}$ for both transverse and longitudinal phonons and also in both class I and class II events. At the same time, it can be seen that at high temperatures $\tau_{3ph,U}^{-1}$ dominates over $\tau_{3ph,N}^{-1}$. As a result, one can say that at low temperature three-phonon N-processes play a dominating role in the estimation of the lattice thermal conductivity of both samples, whereas at high temperatures the lattice thermal resistivity is mainly due to three-phonon U-processes. These findings are in agreement with the findings of the earlier workers [4, 5, 33].

The importance of three-phonon scattering relaxation rates $\tau_{3ph,T}^{-1}$ (class I) and $\tau_{3ph,L}^{-1}$ (Class I + class II) can be studied with the help of Tables 5, 6 and 8, 9 for Mg_2Ge and Mg_2Si, respectively, which show the percentage contributions $\%\,\tau_{3ph,T}^{-1}$ and $\%\,\tau_{3ph,L}^{-1}$ towards the combined scattering relaxation rates $\tau_{c,T}^{-1}$ and $\tau_{c,L}^{-1}$, respectively, in the absence of the four-phonon scattering relaxation rate τ_{4ph}^{-1}. It should be noted that in these Tables, in some places, the contributions are reported as zero. In fact, these are not zero, but a very small quantity. Similarly, in some places we have reported the percentage contributions as 100; these are not 100, but very close to 100. From these Tables, it is clear that at high temperatures τ_{3ph}^{-1} dominates over the point-defect and boundary scattering relaxation rates. As a result, it can be said that at high temperatures the lattice thermal resistivity of a sample is mainly due to phonon-phonon scattering, which is similar to the earlier findings of Mamilton and Parrott [63] based on the variational method. At the same time, it is similar to those reported by Dubey [33, 66] for Si and Ge based on the relaxation time approach. From these Tables, it can be seen that at low temperatures (say below 15 K) the percentage contribution $\%\,\tau_{3ph}^{-1}$ due to the three-phonon scattering relaxation rate is very small, which shows the domination of τ_B^{-1} and $\tau_{p.}^{-1}$ over τ_{3ph}^{-1} at low temperatures. Due to these results, one can say that at low temperatures the lattice thermal resistivity of a sample is mainly due to boundary and point-defect scattering relaxation rates, which is in agreement with the previous findings [38–40, 55].

*

The authors wish to express their thanks to Dr. R. H. Misho for his valuable suggestions. They are also grateful to Dr. A. J. Saleh and Dr. R. A. Rashid for their interest in the present work.

References

1. J. CALLAWAY, Phys. Rev., 113 (1959) 1046.
2. M. G. HOLLAND, Phys. Rev., 132 (1963) 2461.
3. Y. P. JOSHI and G. S. VERMA, Phys. Rev., B1 (1970) 750.
4. P. C. SHARMA, K. S. DUBEY and G. S. VERMA, Phys. Rev., B4 (1971) 1306.
5. K. S. DUBEY and G. S. VERMA, Phys. Rev., B4 (1971) 4491.
6. K. S. DUBEY and R. H. MISHO, J. Thermal Anal., 12 (1977) 223.
7. M. C. AL-EDANI and K. S. DUBEY, Phys. Stat. Solidi, (b)68 (1978) 741.
8. K. C. SOOD, M. A. SINGH and G. S. VERMA, Phys. Rev., B3 (1971) 385.
9. V. V. KASAVEV, P. V. TAMARIN and S. S. SHALYAT, Phys. Stat. Solidi, (b)44 (1971) 525.
10. Y. P. JOSHI, M. D. TIWARI and G. S. VERMA, Phys. Rev., B1 (1970) 642.
11. C. HERRING, Phys. Rev., 95 (1954) 954.
12. P. G. KLEMENS, Solid State Physics (Edited by F. Sertz and D. Turnbull, Academic Press, Inc. New York) 7 (1958) 1.
13. P. G. KLEMENS, Proc. Roy. Soc., London A208 (1951) 108.
14. P. G. KLEMENS, Proc. Phys. Soc., London 68 (1955) 1113.
15. B. K. AGRAWAL and G. S. VERMA, Phys. Rev., 126 (1962) 24.
16. B. K. AGRAWAL and G. S. VERMA, Physica, 28 (1962) 599.
17. A. M. TOXEN, Phys. Rev., 127 (1961 450.
18. K. S. DUBEY, Phys. Rev., B7 (1973) 2876.
19. K. S. DUBEY and G. S. VERMA, B7 (1973) 2879.
20. M. D. TIWARI, D. N. TALWAR and B. K. AGRAWAL, Solid State Comms., 9 (1971) 995.
21. J. J. MARTIN and G. C. DANIELSON, Phys. Rev., 166 (1968) 879.
22. R. H. MISHO and K. S. DUBEY, Ind. J. Pure Appl. Phys., 15 (1977) 48.
23. C. M. BHANDARI and G. S. VERMA, Phys. Rev., 138 (1965) A288.
24. C. M. BHANDARI and G. S. VERMA, Phys. Rev., 140 (1965) A2101.
25. M. D. TIWARI and B. K. AGRAWAL, Phys. Rev., B4, (1971) 4491.
26. K. S. DUBEY, J. Thermal Anal., 20 (1981) 447.
27. K. S. DUBEY, Phys. Stat. Solidi, (b)102 (1980) 423.
28. M. G. HOLLAND, Phys. Rev., 134 (1964) 471.
29. K. S. DUBEY, Ind. J.. Pure Appl. Phys., 13 (1975) 302.
30. M. C. AL-EDANI and K. S. DUBEY, Phys. Stat. Solidi, (b)87 (1978) K47.
31. G. L. GUTHRIE, Phys. Rev., 152 (1966) 801.
32. G. L. GUTHRIE, Phys. Rev., B3 (1971) 3373.
33. K. S. DUBEY, J. Thermal Anal., 19 (1980) 263.
34. I. POMERANCHUK, Phys. Rev., 60 (1941) 820.
35. I. POMERANCHUK, J. Phys. U. S. S. R., 4 (1941) 259.
36. I. POMERANCHUK, J. Phys. U. S. S. R., 7 (1941) 197.
37. LORD RAYLEIGH, Philos. Mag., 36 (1932) 365.
38. H. B. G. CASIMIR, Physica, 5 (1938) 595.
39. R. BERMAN, E. F. SIMON and J. M. JIMAN, Proc. Roy. Soc. London, A220 (1953) 171.
40. R. BERMAN, E. L. FORESTER and J. M. JIMAN, Proc. Roy. Soc. London, A231 (1955) 130.
41. J. CALLAWAY and H. C. BAEVER, Phys. Rev., 120 (1960) 1149.
42. Y. P. JOSHI and G. S. VERMA, Physica, 47 (1970) 213.
43. K. S. DUBEY, J. Physique, France, 37 (1976) 265.
44. K. S. DUBEY, Phys. Stat. Solidi, (b)81 (1977) K83.
45. K. S. DUBEY, Phys. Stat. Solidi, (b)79 (1977) K119.
46. K. S. DUBEY, Solid Stat. Comms., 23 (1977) 963.
47. K. S. DUBEY and G. S. VERMA, Proc. Phys. Soc. Japan, 32 (1971) 1202.
48. A. F. SALEH, R. H. MISHO and K. S. DUBEY, Solid. Stat. Comms.
49. R. M. SAMUAL, R. H. MISHO and K. S. DUBEY, Current Sc., 46 (1977) 220.
50. K. S. DUBEY, Ind. J. Pure Appl. Phys., 11 (1973) 265.
51. J. E. PARROTT, Phys. Stat. Solidi, (b)48 (1971) K159.

52. K. S. DUBEY, Phys. Stat. Solidi, (b)63 (1974) K35.
53. B. K. AGRAWAL and G. S. VERMA, Phys. Rev., 128 (1962) 603.
54. K. S. DUBEY, J. Phys. Chem. Solidi, 39 (1978) 699.
55. P. C. SHARMA, K. S. DUBEY and G. S. VERMA, Phys. Rev., B3 (1971) 1985.
56. P. L. CHUNG, W. B. WHITTEN and G. C. DENIELSON, J. Phys. Chem. Solids, 26 (1965) 1753.
57. K. S. DUBEY, Phys. Rev., B13 (1976) 1836.
58. K. S. DUBEY, Ind. J. Pure. Appl. Phys., 12 (1974).
59. J. J. MARTIN, J. Phys. Chem. Solids, 33 (1972) 1139.
60. W. B. WHITTEN, P. L. CHUNG and G. C. DENIELSON, J. Phys. Chem. Solids, 26 (1975) 49.
61. K. S. DUBEY, J. Thermal Anal., 18 (1980) 35.
62. R. H. MISHO and K. S. DUBEY, Ind. J. Phys., A52 (1977) 234.
63. R. A. H. HAMILTON and J. E. PARROTT, Phys. Rev., 178 (1969) 1284.
64. G. P. SRIVASTAVA, Pramana, 1 (1976) 236.
65. G. P. SRIVASTAVA, Phil. Magn., 34, (1976) 795.
66. K. S. DUBEY, Ind. J. Pure Appl. Phys., 15 (1977) 455.

ZUSAMMENFASSUNG — Die thermischen Gitterleitfähigkeiten von Mg_2Ge und Mg_2Si wurden im ganzen Temperaturbereich von 2 bis 1000 K im Rahmen eines neuen Ausdrucks für die Relaxationsrate der Phonon-Phonon Streuung analysiert, welche von Dubey als

$$\tau_{3ph}^{-1} = (B_{N,I} + B_{U,I}\, e^{-\theta/\alpha T})\, g(\omega)\, T^{m_I(T)} + (B_{N,II} + B_{U,II}\, e^{-\theta/\alpha T})\, g(\omega)\, T^{m_{II}(T)}$$

vorgeschlagen wird, undzwar auf der Guthrie-schen Klassifizierung der Phonon-Phonon Streuung beruhend. Auf diese Weise wurde eine sehr gute Übereinstimmung zwischen den berechneten und experimentellen Werten der thermischen Gitterleitfähigkeit für beide Proben im ganzen Temperaturbereich der Untersuchungen erhalten. Die separaten prozentualen Beiträge, welche den Drei-Phonon Normal- und Umklapp-Prozessen in Richtung der Relaxationsrate der Drei-Phonon-Streuung zuzuschreiben sind, wurden ebenfalls studiert. Die Rolle der Vier-Phonon-Vorgänge wurde in die vorliegende Analyse ebenfalls mit aufgenommen.

Резюме — Для соединений Mg_2Ge и Mg_2Si в области температур 2—1000 К проведен анализ решеточной теплопроводности на основе нового выражения для скорости релаксации фонон-фононного рассеяния, предложенного Дьюби и основанного на классификации Гютри для фонон-фононного рассеяния:

$$\tau_{3ph}^{-1} = (B_{N,I} + B_{U,I}\, e^{-\theta/\alpha T})\, g(\omega)\, T^{m_I(T)} + (B_{N,II} + B_{U,II}\, e)^{-\theta/\alpha T}\, g(\omega)\, T^{m_{II}(T)}$$

Получено хорошее совпадение между вычисленными и экспериментальными значениями решеточной теплопроводности для обоих образцов. Отдельно изучен процентный вклад, вносимый трехфононными нормальными процессами и процессами переброса в релаксационную скорость трехфононного рассеяния. В представленном анализе включена также роль четырехфононных процессов.